Journal of
Flood Risk Management

Benchmarking of flood inundation extent using various dynamically linked one- and two-dimensional approaches

Reza Ahmadian[1], Roger A. Falconer[1] and Jon Wicks[2]

1 School of Engineering, Cardiff University, Cardiff, UK
2 CH2M, Burderop Park, Swindon, UK

Correspondence
Reza Ahmadian, School of Engineering, Cardiff University, Queen's Building, The Parade, Cardiff CF24 3AA, UK.
Email: AhmadianR@cf.ac.uk

DOI: 10.1111/jfr3.12208

Key words
1-D/2-D linking; ADI numerical scheme; flood extent; flood inundation; flood modelling; Greenwich Embayment; TVD numerical scheme.

Abstract

An accurate representation of linking processes between one-dimensional (1-D) and two-dimensional (2-D) models is of particular importance for many flood-modelling projects. This paper provides a comparison of 1-D/2-D linking methods used to simulate a hypothetical embankment failure. Comparisons were made by implementing 1-D/2-D linked models using two different 1-D/2-D linking methods, namely water levels and discharges, using both the alternating direction implicit (ADI) and total variation diminishing (TVD) 2-D numerical schemes widely used in flood models such as Flood Modeller Pro (http://www.floodmodeller.com). The flood inundation levels and extent predicted by each numerical scheme were similar when the discharge method was used to link the models, whereas they were dependent on the numerical scheme when the water-level method was used. Consequently, where decisions affecting public safety are informed by the modelling, such as evacuation following a breach, it is recommended that the discharge-linking method should be used for linking models.

Introduction

Flood risk modelling has attracted considerable interest among researchers and practitioners over the past decades and various one-, two-, three-dimensional (1-D, 2-D and 3-D) and meshless models have been developed for this purpose. In particular, different 2-D models, such as models based on the mass balance equation (Horritt and Bates, 2001), semi-implicit finite-difference solutions of the full 2-D shallow-water equations (Falconer, 1986), explicit finite-difference solutions of the diffusion wave equation (Bradbrook *et al.*, 2004), explicit analytical approximations to the diffusion wave equations (Hunter *et al.*, 2008), explicit finite-difference solutions of the full 2-D shallow-water equations with a total variation diminishing (TVD) solver (Caleffi *et al.*, 2003; Liang *et al.*, 2007b) and explicit finite-volume solutions of the full 2-D shallow-water equations with a Roe Riemann solver (Villanueva and Wright, 2006) have been implemented for flood risk modelling.

Specifically, floodplain modelling has been of particular interest to many researchers and practitioners because such modelling is often a key activity during the processes of developing responses to better manage flood risk. 1-D models are generally regarded as the most appropriate model for representing most aspects of flood behaviour within most river channels and have been used in modelling a wide range of river scenarios (Ervine and MacLeod, 1999; Garcia-Navarro *et al.*, 1999; Werner, 2001). Various research studies have been undertaken to model flooding on a floodplain using extended 1-D models (Horritt and Bates, 2002; Tayefi *et al.*, 2007) and 1-D storage cells (K'uzniar *et al.*, 2002; Faganello and Attewill, 2005; Tayefi *et al.*, 2007; Chatterjee *et al.*, 2008). However, in many cases these models are not fully capable of capturing the flood inundation extent due to limitations inherent in the resolution of 1-D models. Using 2-D models only to simulate flows and elevations in channels and floodplains can require a small grid size to capture all of the bathymetric features of the channel and subsequently can be computationally expensive (Werner, 2001) with the computational time being typically 1000 times greater than that for 1-D models covering a comparable river reach (Wicks *et al.*, 2004). The computational cost is also dependent on the type of 2-D solver utilised in the model as well as the size of the domain and the resolution and the type of grid cells, e.g. higher computational cost is even more apparent when using a nonstructured 2-D grid. Moreover, river boundaries might be far away from the area of interest, which increases the size of the domain and

subsequently the model run time and memory requirements. Furthermore, modelling many hydraulic structures (such as bridges, sluice gates, flood barriers etc.) located in rivers with 2-D models can be challenging, whereas modelling such structures is generally more straightforward in 1-D models. This makes the application of high resolution 2-D models using computationally extensive solvers for real-time flood forecasting less practical. However, the application of high performance computing (HPC), including graphics processor units (GPUs), has shown significant reduction in simulation time (Kalyanapu *et al.*, 2011; Vacondio *et al.*, 2014). Moreover, several approaches such as implementing modified and more complicated 1-D models and application of simplified 2-D models have been used in order to identify efficient ways of simulating flood inundation from riverine sources over floodplains. However, the advances in data availability, improved numerical methods and enhanced computational power have led to an increase in the use of 1-D/2-D linked models to model both the in-river and floodplain hydrodynamic processes.

Tayefi *et al.* (2007) compared 1-D and 1-D/2-D linked approaches to find the most efficient approach to model flood inundation extent over upland reaches of the River Wharfe, UK. They compared three different treatments of flood inundation models. The first method was a 1-D model with the floodplain represented as a sequence of extended cross-sections (referred to as 1-D-E) where 2-D flow in the flood plain was simplified as a 1-D flux between extended cross-sections. The second method, referred to as 1-D-S, consisted of a 1-D model used for the main channel, with the floodplain being represented by a series of storage cells. Based on the floodplain topological characteristics, these storage cells were connected hydraulically to the main river and/or other storage cells. Water levels within cells were calculated by solving only the continuity equation and were assumed to be constant across each cell. Flow exchanges between storage cells and the main channel, and between storage cells, were calculated using the standard equation for a broad-crested weir. The third method, referred to as the 1-D/2-D method, was a theoretically improved form of their 1-D-S method. In this method, instead of splitting the floodplain into a few large storage cells, the floodplain was discretised into a large number of small, regular, storage cells where a 2-D diffusion wave treatment model (Yu and Lane, 2006a,b) was implemented for 2-D modelling of the floodplain. The later approach had a partial treatment of momentum conservation as it was based upon explicit mass conservation and solutions of a simplified form of the shallow-water momentum equations, excluding the spatial and temporal acceleration terms and adopting a Manning friction equation (Bradbrook *et al.*, 2004). They reported that although the 1-D/2-D model produced the best results, both the extended cross-section and the storage cell 1-D models were conceptually problematic. The optimal condition for the main-channel water level for the case of the 1-D/2-D linked model was also the optimal condition for floodplain inundation.

Fang and Su (2006) developed an integrated 1-D and 2-D model to simulate 2-D overland flow and 1-D flow in drainage channels and underground storm water pipes. They applied the model to the City of Beaumont, Texas and treated drainage channels as special flow paths and arranged along one or more sides of a 2-D computational cell. Their model provided good agreement between model predictions and available field data. Dhondia and Stelling (2002) investigated the impact and flooding extent of the Sistan River system, located in the South East of Iran, by successfully implementing a commercial 1-D/2-D linked model. In this model the 1-D model was incorporated within the 2-D mesh and used for a typical 1-D/2-D overtopping study while discharges of 1-D and 2-D models were calculated separately. Liang *et al.* (2007a) compared the Depth Integrated Velocity and Solute Transport (DIVAST) 2-D model to a commercial 1-D model, namely ISIS, and transferred momentum and mass across the interface and obtained satisfactory results for their study. They tested the model for a longitudinal link where the floodplain was located at the end of the 1-D reach and the exchanged flow was calculated using a weir equation.

Lin *et al.* (2006) integrated a 1-D and 2-D models and tested the linked model for idealised test cases, followed by application to the Thames Estuary and the urbanised region of the Greenwich area in London. The 1-D and 2-D models were linked by a weir equation, and comparisons were made between the linked model results and the pseudo-2-D 'flood cell' approach. They demonstrated that differences in flood depths and time of arrival of flood peaks between the two methods were significant. The flood inundation extent predictions using the pseudo-2-D model consisted of many implausible isolated areas of flooding, without any flood route to connect them with the breach site. Finally, they concluded that the linked model predictions were considerably more accurate than the pseudo-2-D 'flood cell' approach. 1-D/2-D linked models have also been used in other studies, such as nondynamic estuarine modelling, where they have been used in predicting flood inundation extent. Umgiesser and Zampato (2001) linked a semi-implicit shallow-water finite element model of Venice Lagoon to a 1-D model of the Venice channel network. This was basically a nondynamic link, where the models could be run separately. Also, a number of researchers have utilised dynamically linked 1-D/2-D models to simulate water quality and suspended sediment (Kashefipour *et al.*, 2002; Ahmadian *et al.*, 2014).

This study mainly focuses on methods available to link 1-D and 2-D models to simulate a lateral embankment over-

Journal of Flood Risk Management published by The Chartered Institution of Water and Environmental Management and John Wiley & Sons Ltd

topping or breach. As discussed earlier, among the methods available to simulate a lateral embankment overtopping or breaching, 1-D/2-D linking can be the most efficient and accurate way of predicting the flood inundation extent for such conditions. The linking replicates the physical processes most appropriately when a weir formulation is used to link the 1-D and 2-D models. However, in this method, a weir effectively has to be introduced for each 2-D cell, which is linked to the river segment. Subsequently, flow between the 1-D and 2-D domains at the link locations will be calculated based on the effective height of the weir (or embankment) and the water levels in the 2-D cell and the river. In practice, this process could be time consuming and, in the interest of simplicity in some cases, the linking is carried out by using the same water levels for the 2-D linked cells (water-level linking). This study focuses on benchmarking these two widely methods using a semi-implicit alternating direction implicit (ADI) method and a shock-capturing TVD numerical scheme for an artificial breach in the Greenwich embankment, London, UK. Ideally a test location where accurate records of boundary conditions and actual inundation extent would have been used; however, such data were not available for this study and comparisons with a 2-D model of the entire domain were not practical because of the size of the domain.

Model development

To develop different linking methods in this study, the open-source DIVAST model, which has been used widely for hydro-environmental studies (Falconer, 1992; Harris *et al.*, 2002; Hunter *et al.*, 2008; Ahmadian *et al.*, 2012), was selected as the 2-D model. This allows implementing different methods and investigating the performance of each method. The ISIS model (subsequently renamed Flood Modeller Pro) was selected as the 1-D model utilised in this study. This was due to the features available in ISIS such as an OpenMI (Moore *et al.*, 2005) compliant structure of the code, which simplified linking, and other modelling features such as including radial gates, which were required for modelling the Thames Barrier.

In order to facilitate efficient linking of the models, the new codes developed for this study, and the existing codes, have been restructured and modified as far as possible to be consistent with OpenMI (Moore *et al.*, 2005). Because OpenMI linking was not the main focus of this study, the developed codes do not include an OpenMI environment, but can easily be changed to be fully compliant with OpenMI. The details of the ISIS model are available at ISIS 1-D (2014), whereas the details of 2-D models, which are the main focus of this study, are described briefly in the next sections.

Numerical schemes

Governing equations

The general conservative form of shallow-water equations can be written as:

$$\frac{\partial \boldsymbol{U}}{\partial \boldsymbol{t}}+\frac{\partial \boldsymbol{E}}{\partial \boldsymbol{x}}+\frac{\partial \boldsymbol{G}}{\partial \boldsymbol{y}}=\frac{\partial \tilde{\boldsymbol{E}}}{\partial \boldsymbol{x}}+\frac{\partial \tilde{\boldsymbol{G}}}{\partial \boldsymbol{y}}+\boldsymbol{S}+T \tag{1}$$

$$\begin{gathered}\boldsymbol{U}=\begin{pmatrix}\boldsymbol{H}\\ \boldsymbol{q_x}\\ \boldsymbol{q_x}\end{pmatrix},\ \boldsymbol{E}=\begin{pmatrix}\boldsymbol{q_x}\\ \frac{\boldsymbol{q_x}^2}{\boldsymbol{H}}+\frac{1}{2}\boldsymbol{gH}^2\\ \frac{\boldsymbol{q_x q_y}}{\boldsymbol{H}}\end{pmatrix},\ \boldsymbol{G}=\begin{pmatrix}\boldsymbol{q_y}\\ \frac{\boldsymbol{q_x q_y}}{\boldsymbol{H}}\\ \frac{\boldsymbol{q_y}^2}{\boldsymbol{H}}+\frac{1}{2}\boldsymbol{gH}^2\end{pmatrix},\\ \tilde{\boldsymbol{E}}=\begin{pmatrix}0\\ \boldsymbol{\tau_{xx}}\\ \boldsymbol{\tau_{yx}}\end{pmatrix},\ \tilde{\boldsymbol{G}}=\begin{pmatrix}0\\ \boldsymbol{\tau_{xy}}\\ \boldsymbol{\tau_{yy}}\end{pmatrix},\ \boldsymbol{S}=\begin{pmatrix}0\\ +\boldsymbol{q_y}f+\boldsymbol{gH}\left(\boldsymbol{S_{bx}}-\boldsymbol{S_{fx}}\right)\\ 0\end{pmatrix},\\ T=\begin{pmatrix}0\\ 0\\ -\boldsymbol{q_x}f+\boldsymbol{gH}\left(\boldsymbol{S_{by}}-\boldsymbol{S_{fy}}\right)\end{pmatrix}\end{gathered} \tag{2}$$

where H = total water depth (m), which is equal to the depth below datum (h) and water levels over the datum (ζ); q_x, q_y = discharge per unit width ($m^3/s/m$) in the x and y directions, respectively; g = gravitational acceleration (m/s^2); τ_{xx}, τ_{xy}, τ_{yx} and τ_{yy} = components of the turbulent shear stress over the plane (N/m^2); f = Coriolis acceleration due to the Earth's rotation; S_{bx} and S_{by} = bed slopes in the x and y directions, respectively (dimensionless); and S_{fx} and S_{fy} = friction slopes in the x and y directions (dimensionless), respectively.

ADI method

The ADI method was first introduced by Peaceman and Rachford (1955) and Douglas (1955). To avoid solving a full 2-D matrix, this method makes use of splitting the time step into two half-time steps and only one dimension is calculated implicitly at each half-time step. The method only requires the inversion of one scalar tri-diagonal matrix at each half-time step. This makes the scheme very cost-effective computationally and therefore the scheme has been used for a wide range of studies (e.g. Stelling *et al.*, 1986; Namiki, 1999; Meselhe and Sotiropoulos, 2000; Ahmadian *et al.*, 2014). Although the scheme is fairly accurate and cost-effective, the scheme does not respond very well to discontinuities such as hydraulic jumps or dam breaks. More details about the model using the ADI method can be found in Ahmadian *et al.* (2010), Kashefipour *et al.* (2002) and Falconer (1992).

TVD method

The TVD schemes limit the oscillations by implementing nonlinear artificial dissipation and subsequently preserve monotonicity for schemes of higher than first order (Mingham *et al.*, 2001). This makes these schemes applicable to practical cases with a discontinuity such as dam break. In this study the TVD–MacCormack scheme was implemented, which is a TVD version of the second order accurate classical shock-capturing scheme of the MacCormack type. The model implements the scheme proposed by Liang *et al.* (2006), which is explained briefly below for completeness only, with further details being given in Mingham *et al.* (2001) and Liang *et al.* (2006). Rogers *et al.* (2003) presented that the general conservative form of SWE equations (Eqns 1 and 2) and after neglecting the diffusion terms and the Coriolis force could be written as follows:

$$\frac{\partial \boldsymbol{U}}{\partial t}+\frac{\partial \boldsymbol{E}}{\partial x}+\frac{\partial \boldsymbol{G}}{\partial y}=\boldsymbol{S}+T \tag{3}$$

$$\boldsymbol{X}=\begin{pmatrix}\xi\\ q_x\\ q_x\end{pmatrix},\ \boldsymbol{E}=\begin{pmatrix}q_x\\ \frac{q_x^{\,2}}{\xi+h}+\frac{1}{2}g\xi^2+gh\xi\\ \frac{q_xq_y}{\xi+h}\end{pmatrix},$$

$$\boldsymbol{G}=\begin{pmatrix}q_y\\ \frac{q_xq_y}{\xi+h}\\ \frac{q_y^{\,2}}{\xi+h}+\frac{1}{2}g\xi^2+gh\xi\end{pmatrix},\ \boldsymbol{S}=\begin{pmatrix}0\\ g\xi\frac{\partial h}{\partial x}-\frac{gq_x\sqrt{q_x^{\,2}+q_y^{\,2}}}{(h+\xi)^2C^2}\\ 0\end{pmatrix},$$

$$T=\begin{pmatrix}0\\ 0\\ g\xi\frac{\partial h}{\partial y}-\frac{gq_y\sqrt{q_x^{\,2}+q_y^{\,2}}}{(h+\xi)^2C^2}\end{pmatrix} \tag{4}$$

Equation 3 was solved using the Strang operator (Strang, 1968) splitting technique, which simplifies the solution procedure by changing the 2-D problem to two 1-D problems, which are solved in sequence, as shown below:

$$\frac{\partial X}{\partial t}+\frac{\partial F}{\partial x}=S \tag{5}$$

$$\frac{\partial X}{\partial t}+\frac{\partial G}{\partial y}=T \tag{6}$$

For a regular rectangular grid, as used in this study, Eqns (5) and (6) can be written as:

$$X_{i,j}^{n+1}=L_xX_{i,j}^{n} \tag{7}$$

$$X_{i,j}^{n+1}=L_yX_{i,j}^{n} \tag{8}$$

where L_x and L_y are the finite-difference operators and subscript and the superscript for X denote the corresponding grid cell location and time level, respectively. For each time step the TVD–MacCormack scheme is used to solve the two 1-D hyperbolic equations consecutively at each time step. The discretisation scheme for Eqn (7), gives:

$$X_i^{p}=X_i^{n}-\left(F_i^{n}-F_{i-1}^{n}\right)\cdot\frac{\Delta t}{\Delta x}+S^{n}\cdot\Delta t \tag{9}$$

$$X_i^{c}=X_i^{n}-\left(F_{i+1}^{p}-F_i^{p}\right)\cdot\frac{\Delta t}{\Delta x}+S^{p}\cdot\Delta t \tag{10}$$

$$X_i^{n+1}=\frac{1}{2}\cdot\left(X_i^{p}+X_i^{c}\right)-TVD_i^{n} \tag{11}$$

where Δx = grid size, Δt = time step and the superscripts p and c represent the predictor and corrector steps, respectively. Using the predictor-corrector method guarantees second-order accuracy in both space and time. TVD_i^n = an extra TVD term added to the standard MacCormack scheme, where:

$$TVD_i^{n}=\left[G\left(r_i^{+}\right)+G\left(r_i^{-}\right)\right]\cdot\Delta X_{i+\frac{1}{2}}^{n}-\left[G\left(r_{i-1}^{+}\right)+G\left(r_i^{-}\right)\right]\cdot\Delta X_{i-\frac{1}{2}}^{n} \tag{12}$$

where $G(\ )$ = a function dependent on the wavespeed direction and flux limiter function and r values are dependent on gradients around the solution cell. Using the TVD term ensures that the numerical oscillations near the sharp-gradient regions are removed.

Model setup

1-D model setup

The data for the 1-D model of the Thames River used for this study were provided by CH2M Ltd. The model starts at Molesey, upstream of the Teddington Weir Complex, and ended in the Thames Estuary. The model was approximately 110 km long and included 121 cross-sections. The bed elevation of the cross-sections across the domain changes from 1.38 m AOD to −19.2 m AOD. Radial and vertical sluice gates, spills, weirs and gated weirs were used to control the flow condition in the model reach, including Teddington sluices, Richmond Locks and the Thames Barrier. Figure 1 illustrates the extent of the 1-D model domain including the Greenwich Embayment.

The upstream boundary condition consisted of a constant flow of 200 $m^3\ s^{-1}$, representing a typical flow for the River

Journal of Flood Risk Management published by The Chartered Institution of Water and Environmental Management and John Wiley & Sons Ltd

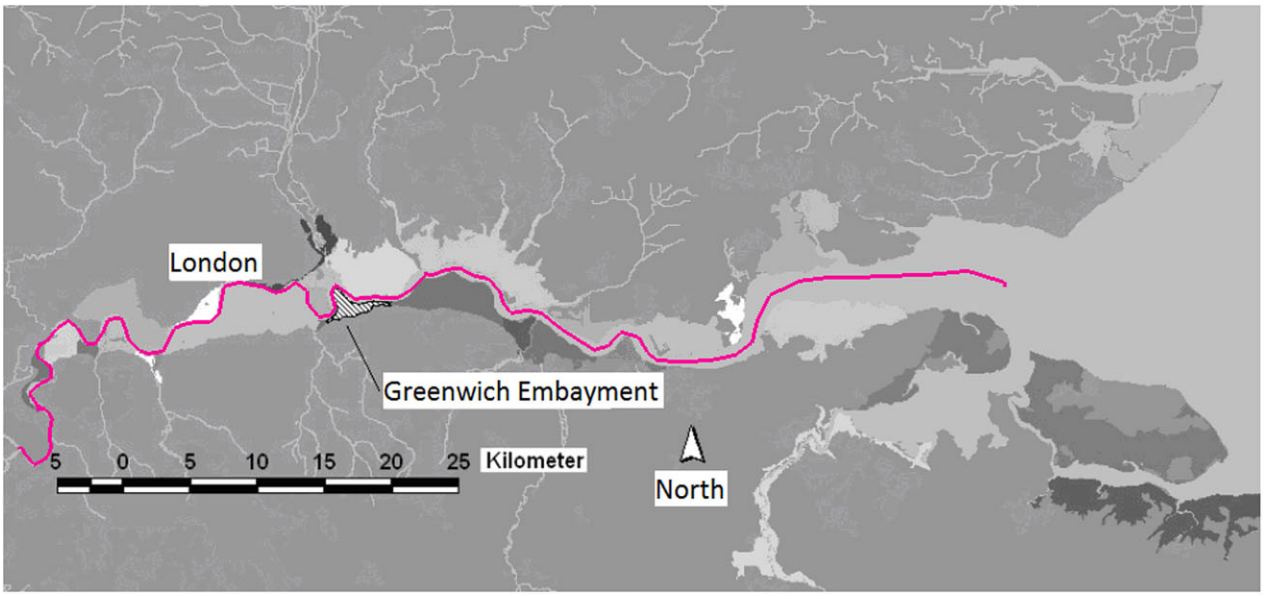

Figure 1 Thames tidal embayment, including Greenwich embayment, and the 1-D model cross-sections centreline (magenta Line) – Source of the background picture: Lin *et al*. (2006).

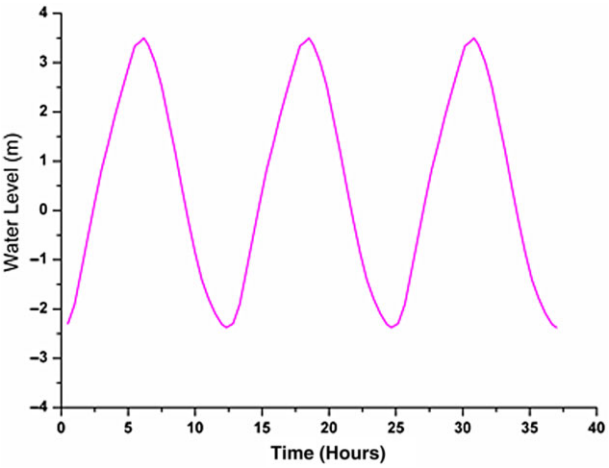

Figure 2 Downstream boundary for the 1-D model.

Thames, with the downstream boundary condition consisting of the tidal water levels, as illustrated in Figure 2.

Figure 3 illustrates the predicted water levels along the 1-D domain after 20 hours from the start of simulation acquired by using the standalone 1-D model without linking to the 2-D model.

2-D model

The Greenwich Embayment was chosen as the main area of interest for the 2-D modelling. Figure 4 depicts the extent of the 2-D model and the 1-D model cross-sections, including components of the Thames barrier, as well as the location of the artificial breach where the 1-D and 2-D models were linked. The 2-D model was built using a 5×5 m^2 mesh, with the bed elevations being derived from the topography obtained using Light Detection and Ranging (LiDAR) data provided by the Environment Agency of England 4.

The buildings were treated as solid blocks with no water being allowed to flow into the buildings. The Manning's number was set to 0.030, and it was assumed that the only source or sink of water in the 2-D domain was via the link with the 1-D model.

Linking

Although ISIS is a commercial code because it is compatible with an OpenMI standard, the functions and subroutines needed to link the model were accessible and exposed in a dynamic link library (DLL) file, i.e. ISIS_OMI.DLL. Dynamic linking of the 1-D and 2-D models was achieved using ISIS_OMI.DLL and a similar DLL developed for the 2-D model and following a structure compatible with ISIS_OMI.DLL.

A flood event was artificially created by setting a synthetic embankment breach. A breach was set at an arbitrary location along the embankments on the west side of the 2-D model domain as illustrated in Figure 4b.

In linking the models using water-level linking, the 2-D linked cells were treated as water-level boundaries. Their values were derived from the water levels along the 1-D reach adjacent to these cells. The water mass added or removed from these cells, and through the link, was calculated at each time step and was communicated to the hydrograph associated

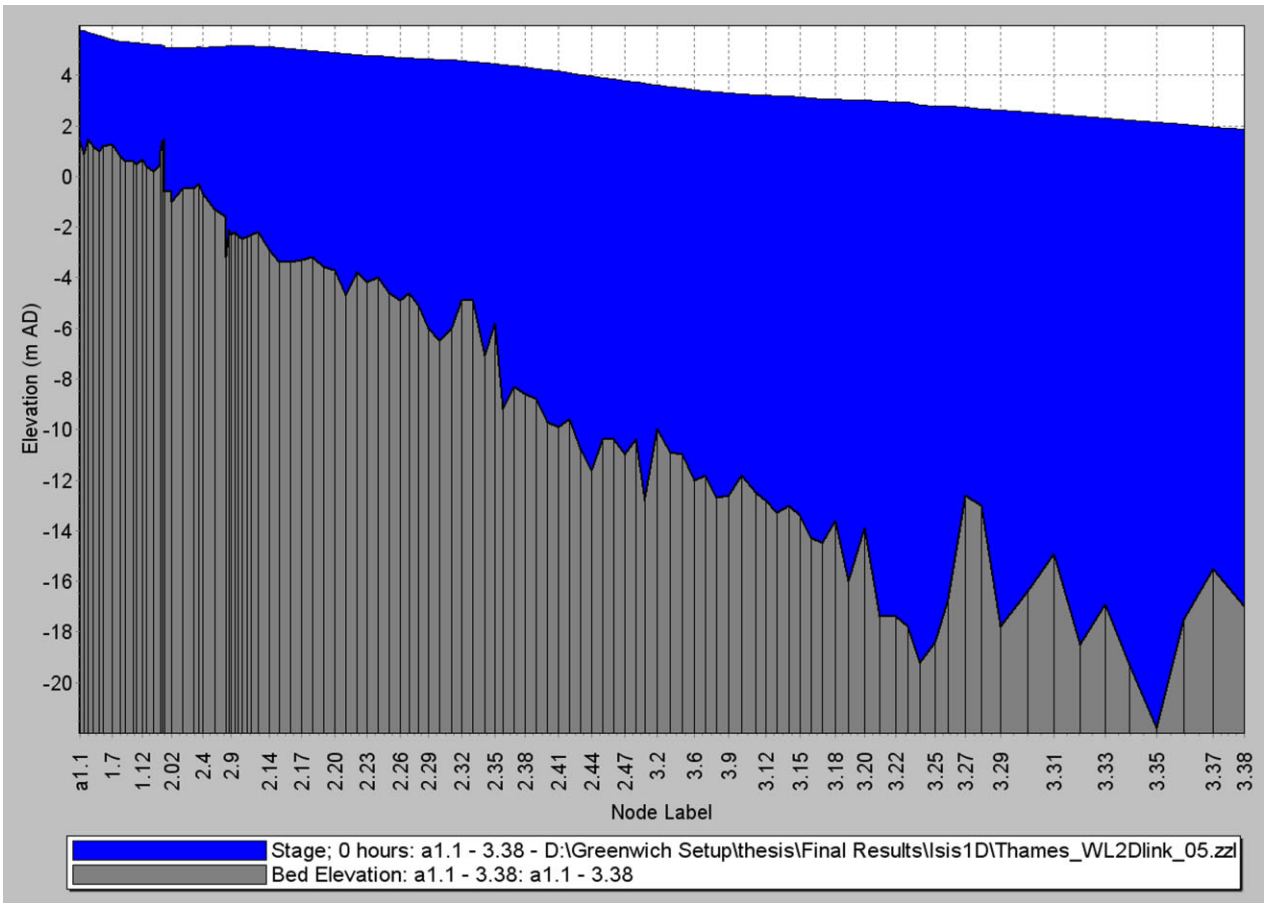

Figure 3 Predicted water levels along the 1-D domain after 20 hours from the start of simulation.

with the corresponding 1-D reach. This method does not noticeably interfere with the 1-D model simulations.

Linking the models by utilising discharge involves simulating the over bank flow from the river to floodplain using a weir equation. This is a more elaborative and complex procedure. In this method, a number of lateral weirs were defined along the 1-D reach where the breach was expected to occur. To simulate a breach, the height of the weirs were initially set to the height of the flood defences and when breach was expected to occur these levels were adjusted to the anticipated height of the breach. Water levels on either side of these weirs were derived from the corresponding water levels in the 1-D reach and adjacent 2-D cells. The flow through the link depended on these water levels in the linked 2-D cells and 1-D cross-section as well as the height of the weir. However, the water levels in the 2-D cells used for linking and the height of the flood defence, which would be used to determine the height of the weir, could vary significantly along the breach site and these variations could therefore affect the flow over the weir considerably. Therefore, in order to simulate the flow over the weir accurately, it was found to be very important that the length of the weir was not much longer than the 2-D cell dimensions and only a very limited number of cells were linked to each weir. This, in turn, required adding a large number of weirs if a large number of cells were used to simulate the link. Subsequently this made setting up of the model using discharge links more time consuming and elaborative than the water-level links version.

Because the breach was hypothetical in this study, a short breach with the length of only 10 m was considered, and the length and depth of the breach was treated to be constant during the simulation. However, depending on the material of the embankment, significant scour has often been identified at the breach location (Hudson *et al.*, 2008), such changes in the bathymetry inevitably leading to a larger breach area and hydrodynamic conditions immediately downstream of such a breach.

The artificial breach occurred between cross-sections 2.43 and 2.44 of the 1-D model and close to cross-section 2.44 as shown in Figure 4. In considering the 10 m length of the breach and the 5 m 2-D model grid size, then only two cells from the 2-D domain were linked to the 1-D model domain. The height of the embankment, which acted as a flood

Journal of Flood Risk Management published by The Chartered Institution of Water and Environmental Management and John Wiley & Sons Ltd

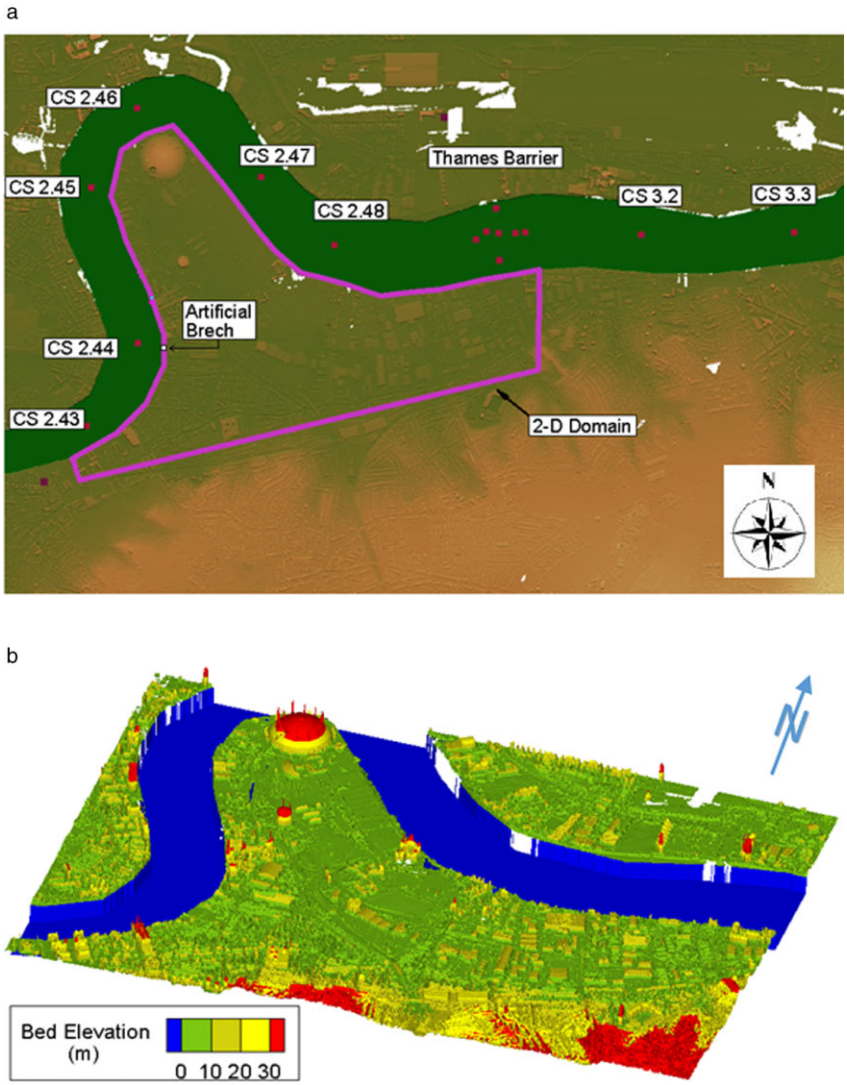

Figure 4 (a) The extent of the 2-D model (magenta polygon), the 1-D/2-D link location and the 1-D model cross-sections and elements around the Greenwich embayment (red squares); (b) 3-D view of the Greenwich Embayment (white areas show areas where no elevation data were available).

defence in the region of the artificial breach, was initially 5.48 m. It was assumed that the height of the flood defence after the breach was reduced to 3.75 m AOD.

Using the water-level linking method, the linked cells in the 2-D model were flagged as water-level boundary cells. The height of the western side of these linked cells in the 2-D model were reduced to 3.75 m AOD and the water levels in these cells were set to the levels derived from the reach between cross-sections 2.43 and 2.44 of the 1-D model. The flow in or out of the 2-D domain, as a result of the imposed water-level boundary, was calculated from the 2-D model. In implementing the discharge-linking method, the linked cells within the 2-D model were flagged as discharge boundary cells. Two lateral weirs, with a length of 5 m each, were introduced between cross-sections 2.43 and 2.44 of the 1-D model. The height of these weirs were initially set to 5.48 m and were then reduced to 3.75 m AOD after the breach and linked to the adjacent 2-D cells. The discharge transferred between the models was calculated by implementing the ISIS broad-crested weir function using water levels from the corresponding 2-D cells and 1-D cross-section. This function includes both modular and nonmodular wires, and the coefficient of velocity, i.e. C_v, was set to 1. More information on the ISIS broad-crested weir function can be found in the ISIS manual (ISIS 1-D, 2014).To conserve mass in the 1-D model, the volume of water entering or exiting the 2-D domain was subtracted or added to the reach using a hydrograph linked to the reach between cross-sections 2.43 and 2.44.

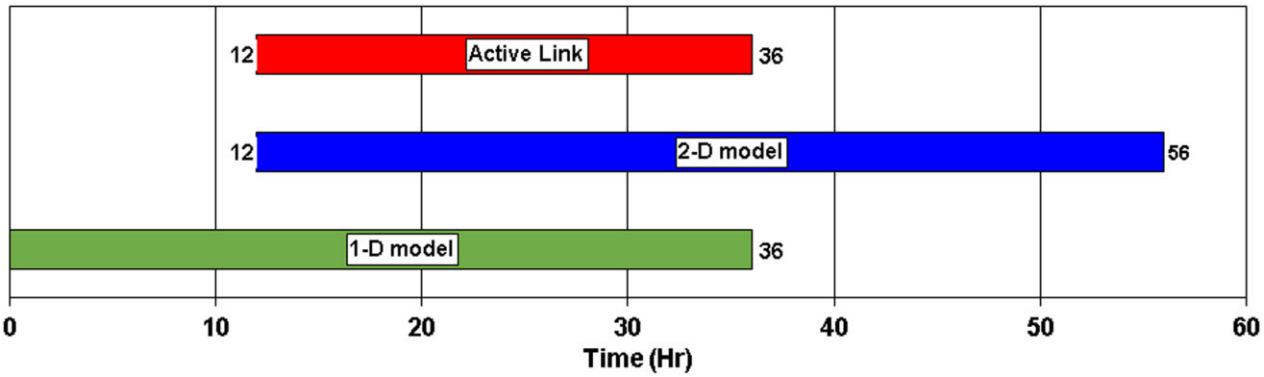

Figure 5 1-D and 2-D model simulation, and link time. Green bar: 1-D model simulation time. Blue bar: 2-D model simulation time. Red bar: linked model simulation time.

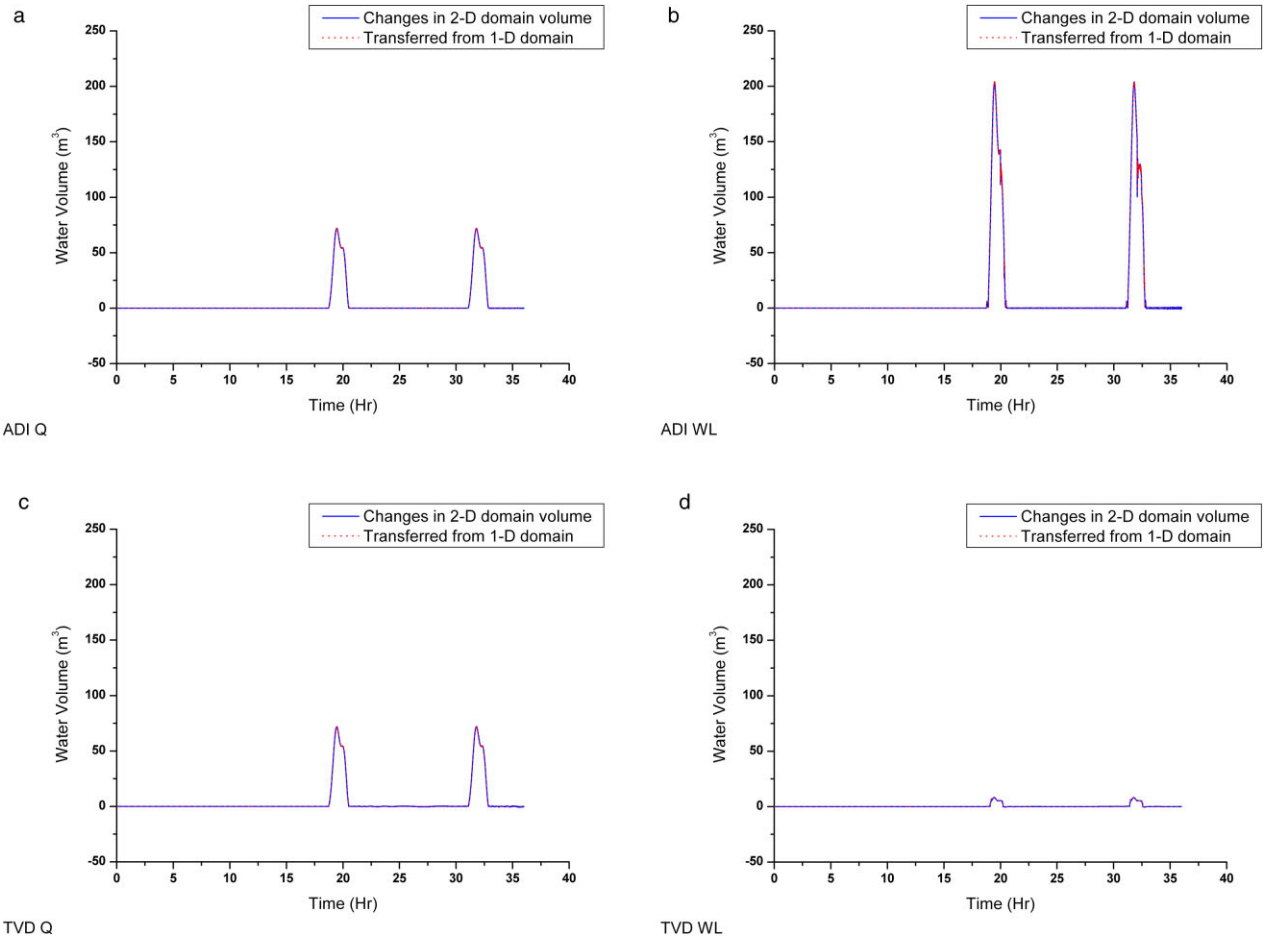

Figure 6 Mass conservation through the link for different linking methods and 2-D models; (a) alternating direction implicit with discharge link (ADI-Q), (b) alternating direction implicit with water-level link (ADI-WL), (c) total variation diminishing with discharge link (TVD-Q), (d) total variation diminishing with water-level link (TVD-WL).

Figure 5 shows the timing of the different models, 12 hours (i.e. almost one tidal cycle) ramping period was used for the 1-D model and therefore the 1-D model was run in this period without being linked to the 2-D model. This was done so the initial instabilities in the 1-D model were passed and the model became stable before linking. The artificial breach was designed to occur after 12 hours and the link between the 1-D and 2-D models was activated. The models

Figure 7 Monitoring point locations across the 2-D domain.

were linked for 24 hours (i.e. 36 hours from the beginning of the simulation period), and after this time the artificial breach was removed and the elevation of flood defences reverted to the initial elevation, namely 5.48 m. The 2-D model was run for 20 hours after the breach was removed, allowing the flow to spread across the 2-D domain.

Results and discussion

The results for both the ADI and TVD schemes using the water-level and discharge links are presented in this section. For convenience, the ADI schemes with water-level and discharge links are denoted as ADI-WL and ADI-Q respectively, whereas the TVD schemes with water-level and discharge links are denoted as TVD-WL and TVD-Q, respectively. The time referred to in the results reported herein is the time from the beginning of the simulation period. By observing the water levels in the standalone 1-D model in the vicinity of the breach location, it was found that the water levels in the river reach above the breach level, namely 3.75 m AOD, occurred almost 6.5 hours after the link was activated. This corresponded to about 18.5 hours from the beginning of the simulation period, which was observed throughout the results.

The first step was to investigate the ability of the link in conserving fluid mass. This was carried out by comparing the water volume transferred from, or to, the 1-D model and the corresponding changes in the volume of water in the 2-D model. Because there was no water in the 2-D domain prior to the existence of the link, it was assumed that the water exchanged with the 1-D domain should be equal to the changes to the water volume in the 2-D domain. Figure 6 illustrates the mass balance, in the form of a volume balance and a constant density, for the ADI-Q, ADI-WL, TVD-Q and TVD-WL models.

Figure 6 illustrates that all four models demonstrated a good mass balance, with no changes in the volume of water transferred between the models. This figure also shows that the water entering the 2-D domain using a discharge link has followed a similar trend regardless of the numerical scheme used for the 2-D domain. However, the results for the ADI-WL model show that much more water has entered the 2-D domain using this method in comparison with the volume of water entering the 2-D domain for the other methods considered. The maximum volume of water entering the 2-D domain using the ADI-WL model was more than 20-fold larger than the maximum water volume entering the domain using the TVD-WL model.

To understand the flood inundation extent using different methods, water depths for all of the schemes were monitored at various locations inside the 2-D domain. The location of some of these monitoring points, which were more relevant to this study, is illustrated in Figure 7. Typical comparisons of the predicted water depths obtained using water-level and discharge links, for both the ADI and TVD schemes, are shown for these points in Figure 8.

Figure 8 demonstrates that the water depths predicted using the ADI-WL model were larger, with a greater inundation extent than the depths and inundation extent predicted for the other schemes. This can be seen from the larger water depths at all points as well as the inundation extents at locations 4, 7 and 9 where all of the other models do not

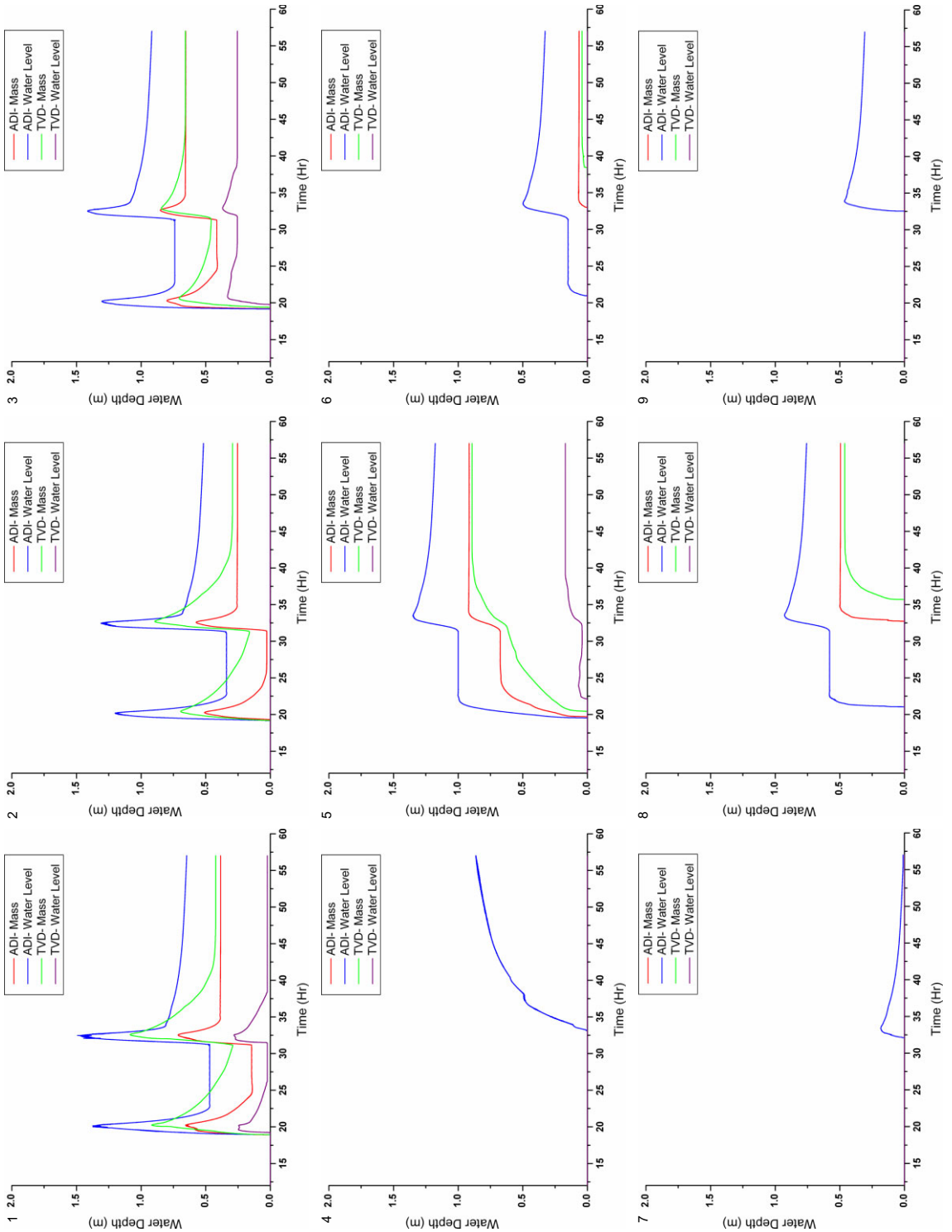

Figure 8 Predicted water depth at various locations across the domain of interest for all four scenarios, namely alternating direction implicit with water-level link (ADI- WL), alternating direction implicit with discharge link (ADI-Q), total variation diminishing with water-level link (TVD-WL) and total variation diminishing with discharge link (TVD-Q) (density was assumed to be constant).

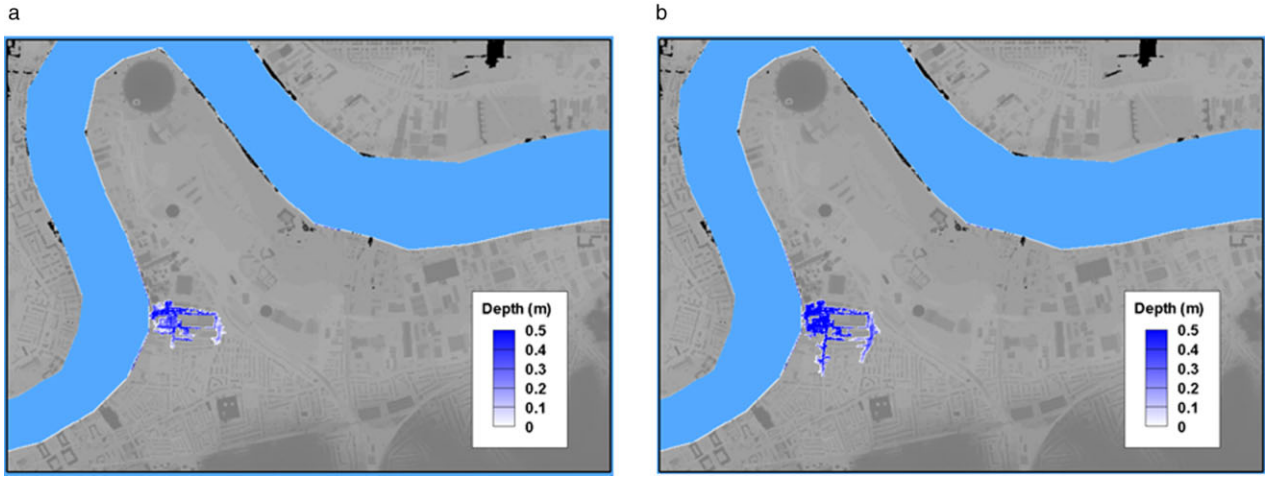

Figure 9 Water depths (m) predicted at time = 19.5 hours using the alternating direction implicit scheme: (a) discharge link and (b) water-level link.

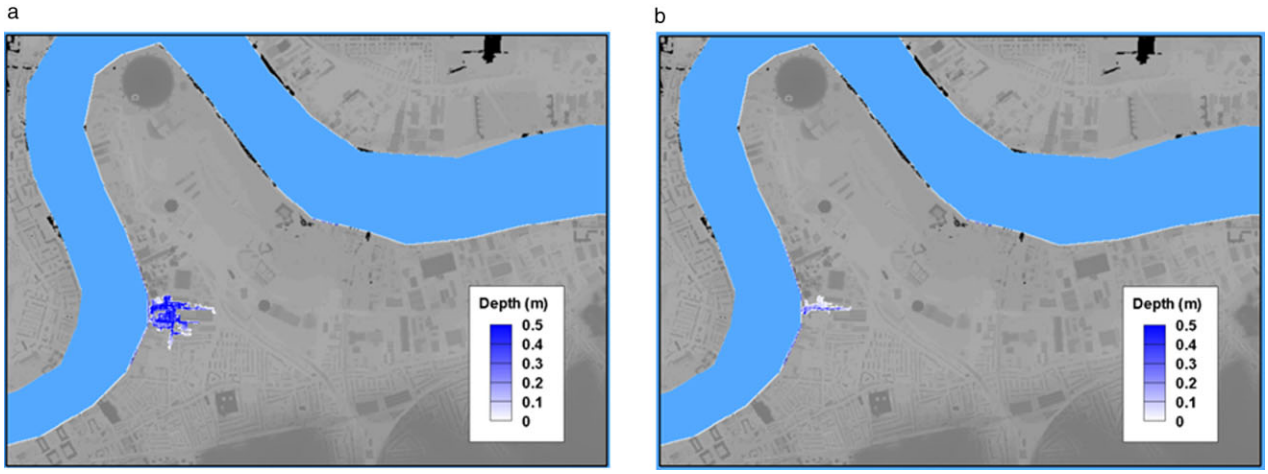

Figure 10 Water depths (m) predicted at time = 19.5 hours using the total variation diminishing scheme: (a) discharge link and (b) water-level link.

predict any flooding at these locations. It is also of importance that both the ADI and TVD schemes with a discharge link exhibit similar inundation extent at the end of the simulation period. However, a comparison of the predictions obtained using these two methods, namely the TVD-Q and ADI-Q, shows that the flood spread out more quickly when the ADI-Q method was used. This is shown in the predicted depths at locations 5, 6 and 8, where the water depth rose faster with the ADI-Q method in comparison with the TVD-Q method, whereas the final levels were similar. This faster spreading of floods for the ADI-Q method can also be seen by comparing the slightly deeper inundation levels predicted using the TVD-Q method in the vicinity of the link location, namely at points 1, 2 and 3, with comparisons being made with the ADI-Q method. This is thought to be related to the excessive artificial diffusion, which is inherently added to implicit models for high Froude number flows. Finally, the water depths predicted using the TVD-WL model were shown to be shallower than the depths predicted using the other methods.

The flood inundation extent predicted across the domain using the water-level and discharge links, for both the ADI and TVD models, and 19.5 and 38.5 hours after the start of the simulations, is illustrated in Figures 9–12.

Figures 9–12 illustrate the differences in the flood inundation extent predicted for each scheme, while also highlighting that the flood path predicted using all of the schemes were similar. As for the water levels at the monitoring points, the ADI-WL method predicted a much larger flood inundation extent with time across the domain, in

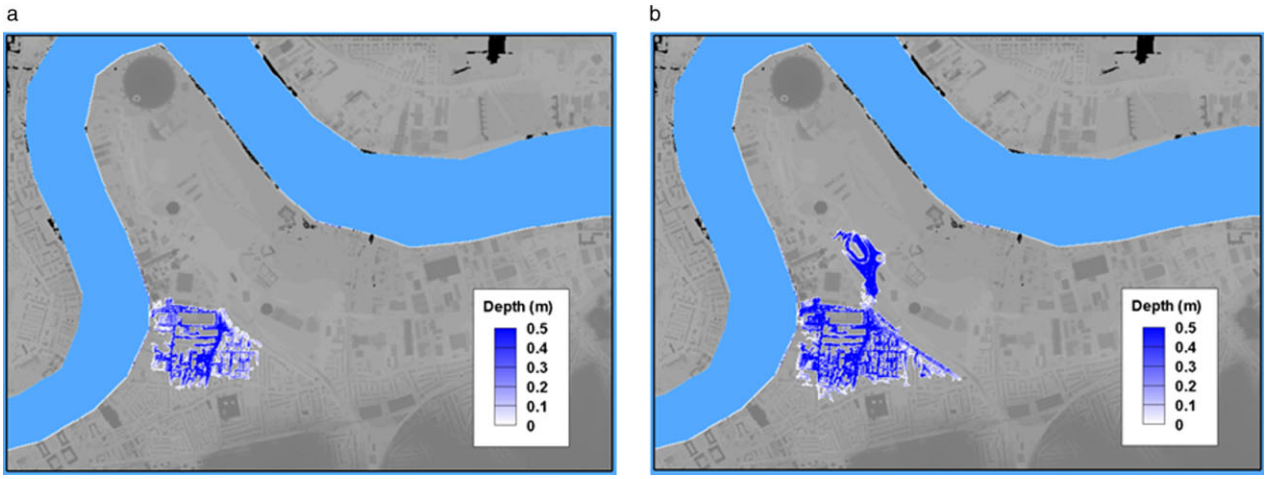

Figure 11 Water depths (m) predicted at time = 38.5 hours using the alternating direction implicit scheme: (a) discharge link and (b) water-level link.

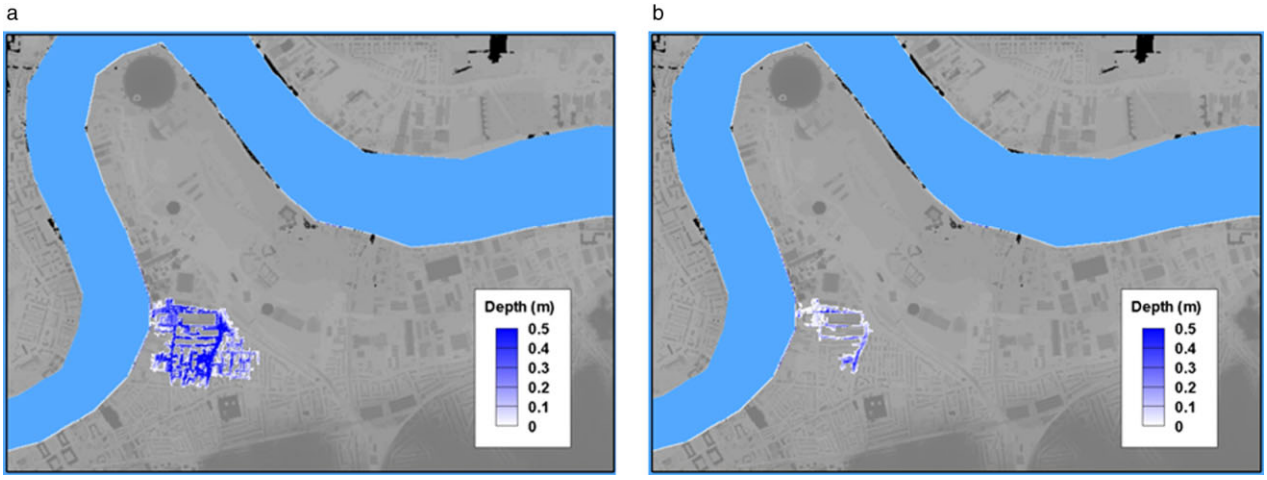

Figure 12 Water depths (m) predicted at time = 38.5 hours using the total variation diminishing scheme: (a) discharge link and (b) water-level link.

comparison with the other methods, whereas the TVD-WL method predicted the smallest flood inundation extent. The flood inundation extent predicted using discharge link (Q) for both ADI and TVD schemes is very similar, although the ADI scheme predicted flood extents are slightly larger.

The number of wet cells, where the depth of water was greater than the flooding and drying threshold of 5 cm, over the simulation period, for each scheme is shown in Figure 13. Moreover, Table 1 highlights the total number of wet cells, the volume inside the domain and the average water depth across the domain, calculated by dividing the basin volume by the number of wet cells, at the end of the simulation period. Similarly, as before, Figure 13 and Table 1 show that the largest area flooded was predicted using ADI-WL method, with the smallest flooded area occurring for the TVD-WL method. The final number of wet cells predicted using the ADI-Q, TVD-Q and TVD-WL methods were 55%, 54% and 14% of the number of wet cells predicted using the ADI-WL method, respectively. Although the ADI-Q method showed a slightly larger flood inundation extent in comparison with the TVD-Q scheme, the water volume within the basin using the ADI-Q method was slightly less than that predicting using the TVD-Q method. Furthermore, the average depth predicted using the ADI-Q method was slightly less than that predicted using the TVD-Q method, which is considered to be negligible.

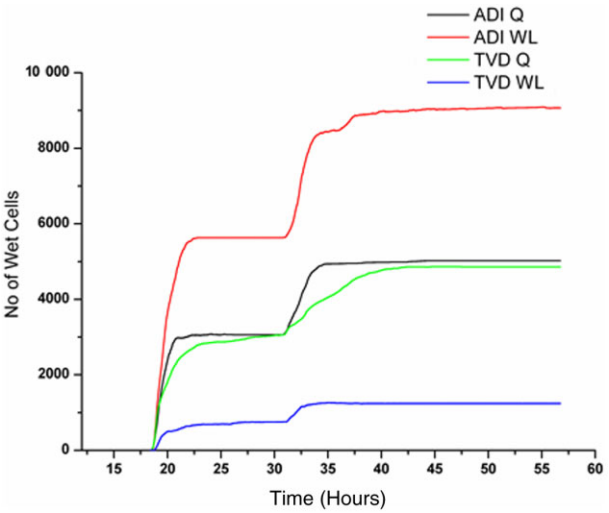

Figure 13 Number of wet cells over time across the domain.

Table 1 2-D domain flood characteristics

Model	ADI-Q	ADI-WL	TVD-Q	TVD-WL
No. of wet cells	5 023	9 069	4 860	1305
2-D domain water volume (m^3)	53 750	132 318	53 842	4925
Wet area average depth (m)	0.428	0.584	0.443	0.151

2-D, two-dimensional; ADI-Q, alternating direction implicit with discharge link; ADI-WL, alternating direction implicit with water-level link; TVD-Q, total variation diminishing with discharge link; TVD-WL, total variation diminishing with water-level link.

Conclusions

A 1-D model of the River Thames was dynamically linked to a 2-D model of the Greenwich Peninsular, located in London, UK, to predict flood extents following a hypothetical breach of the flood defences. The models were linked using water levels and discharge-linking methods, with the ADI and TVD numerical schemes utilised to solve the governing equations in the 2-D model. The link between the models is structured to comply with the OPEN-MI standard.

It was found that water level and discharge links produced very different results, regardless of the numerical schemes used in that scenario. When the ADI-WL model was utilised, the flow spread out faster and inundated larger areas of the domain in comparison with the results obtained for the other methods considered. The TVD-WL model predicted the least amount of water propagating across the breach and into the domain and, in turn, the smallest flooded area. These results show significant differences in the amount of water entering the 2-D domain from the 1-D model, and consequently significant differences were also predicted in the flood inundation extent when using a water-level link with each of the ADI and TVD numerical schemes. In contrast, both the ADI and TVD numerical schemes produced similar results when a discharge link was implemented. However, the flow spread slightly faster when the ADI scheme was used. Discrepancies in the flood inundation extent were predicted between the ADI and TVD schemes and when the 1-D and 2-D domains were linked using the water-level method, which indicated that the water-level linking method should be used with caution in applications where public safety is a consideration, for example for evacuation planning following breach of flood defences. In comparison, the similarity in the results when the discharge-linking approach was used highlights the consistency and potential-improved accuracy in the predicted results when the discharge-linking method is used in simulating embankment breach or failure. The lack of observed flood observations means that it is not possible to quantify the accuracy of the different methods tested and therefore the interpretation of the results provided above would benefit from further field data for the future.

Acknowledgement

The authors thank CH2M staff who provided data, insight and expertise that greatly assisted the research. The Environment Agency of England is thanked for providing data. The analysis was undertaken by the first two authors and does not necessarily reflect the views of CH2M or the Environment Agency.

References

Ahmadian R., Falconer R.A. & Lin B. Hydro-environmental modelling of proposed Severn barrage, UK. *P I Civil Eng.-Energ* 2010, **163**, 107–117.

Ahmadian R., Falconer R. & Bockelmann-Evans B. Far-field modelling of the hydro-environmental impact of tidal stream turbines. *Renewable Energ* 2012, **38**, 107–116.

Ahmadian R., Falconer R.A. & Bockelmann-Evans B. Comparison of hydro-environmental impacts for ebb-only and two-way generation for a Severn Barrage. *Computers Geosci* 2014, **71**, 11–19.

Bradbrook K.F., Lane S.N., Waller S.G. & Bates P.D. Two dimensional diffusion wave modelling of flood inundation using a simplified channel representation. *Int J River Basin Manag* 2004, **2**, 211–223.

Caleffi V., Valiani A. & Zanni A. Finite volume method for simulating extreme flood events in natural channels. *J Hydraulic Res* 2003, **41**, 167–177.

Chatterjee C., Förster S. & Bronstert A. Comparison of hydrodynamic models of different complexities to model floods with emergency storage areas. *Hydrol Proc* 2008, **22**, 4695–4709.

Dhondia Z. & Stelling G. Application of one-dimensional–two-dimensional integrated hydraulic model for flood simulation and damage assessment. International Conference on Hydroinformatics, UK, 2002, pp. 265–276.

Douglas J.J., 1955. On the numerical integration of ∂2u/∂x2 + ∂2u/∂y2 = ∂u/∂t by implicit methods. *J Soc Indust Appl Mathem* **3**, pp. 42–65.

Ervine A. & MacLeod A.B. Modelling a river channel with distant floodbanks. *Proceedings of the ICE – Water Maritime and Energy*, 1999, pp. 21–33.

Faganello E. & Attewill L. Flood management strategy for the upper and middle Odra River Basin: feasibility study of Raciborz Reservoir. *Nat Hazard* 2005, **36**, 273–295.

Falconer R.A. Water quality simulation study of a natural harbor. *J Waterway, Port, Coastal and Ocean Eng* 1986, **112**, 15–34.

Falconer R.A. Research developments of flow and water-quality modeling in coastal and estuarine waters. In *Water Quality Modelling*. R.A. Falconer ed. Aldershot, UK: Ashgate Publishing Co., 1992, pp. 81–109.

Fang X. & Su D. An integrated one-dimensional and two-dimensional urban stormwater flood simulation model. *JAWRA* 2006, **42**, 713–724.

Garcia-Navarro P., Fras A. & Villanueva I. Dam-break flow simulation: some results for one-dimensional models of real cases. *J Hydrol* 1999, **216**, 227–247.

Harris E., Falconer R.A., Kay D. & Stapleton C. Development of a modelling tool to quantify faecal indicator levels in Cardiff Bay. *Proc Inst Civ Eng Water Marit Eng* 2002, **154**, 129–135.

Horritt M.S. & Bates P.D. Effects of spatial resolution on a raster based model of flood flow. *J Hydrol* 2001, **253**, 239–249.

Horritt M.S. & Bates P.D. Evaluation of 1D and 2D numerical models for predicting river flood inundation. *J Hydrol* 2002, **268**, 87–99.

Hudson P.F., Middelkoop H. & Stouthamer E. Flood management along the Lower Mississippi and Rhine Rivers (the Netherlands) and the continuum of geomorphic adjustment. *Geomorphology* 2008, **101**, 209–236.

Hunter N.M., Bates P.D., Neelz S., Pender G., Villanueva I., Wright N.G., Liang D., Falconer R.A., Lin B., Waller S., Crossley A.J. & Mason D.C. Benchmarking 2D hydraulic models for urban flooding. *Proceedings of the ICE – Water Management*, 2008, pp. 13–30.

ISIS 1-D. ISIS 1D, 2014. CH2M.

Kalyanapu A.J., Shankar S., Pardyjak E.R., Judi D.R. & Burian S.J. Assessment of GPU computational enhancement to a 2D flood model. *Environ Model Softw* 2011, **26**, 1009–1016.

Kashefipour S.M., Lin B., Harris E. & Falconer R.A. Hydro-environmental modelling for bathing water compliance of an estuarine basin. *Water Res* 2002, **36**, 1854–1868.

K'uzniar P., Popek Z. & Zelazo J. The analysis of possibility of flood risk decreasing on the Middle Vistula River reach.5th International Conference on Hydro -Science & -Engineering, Warsaw, Poland, 2002.

Liang D., Falconer R.A. & Lin B. Comparison between TVD-MacCormack and ADI-type solvers of the shallow water equations. *Adv in Water Resour* 2006, **29**, 1833–1845.

Liang D., Falconer R.A. & Lin B. Linking one- and two-dimensional models for free surface flows. *Proceedings of the ICE – Water Management*, 2007a, pp. 145–151.

Liang D., Lin B. & Falconer R.A. Simulation of rapidly varying flow using an efficient TVD–MacCormack scheme. *Int J Numer Methods Fluids* 2007b, **53**, 811–826.

Lin B., Wicks J.M., Falconer R.A. & Adams K. Integrating 1D and 2D hydrodynamic models for flood simulation. *Proceedings of the ICE – Water Management*, 2006, pp. 19–25.

Meselhe E.A. & Sotiropoulos F. Three-dimensional numerical model for open-ehannels with free-surfaee variations. *J Hydraulic Res* 2000, **38**, 115–121.

Mingham C.G., Causon D.M. & Ingram D.M. A TVD MacCormacc scheme for transcritical flow. *Proc Inst Civ Eng Water Marit Eng* 2001, **148**, 167–175.

Moore R.V., Gijsbers P., Fortune D., Gregersen J. & Blind M. OpenMI Document Series: Part A – Scope for the OpenMI (Version 1.0). IT Frameworks (HarmonIT) Contract EVK1-CT-2001-00090, 2005, In: Tindall, C.I. (Ed.).

Namiki T. A new FDTD algorithm based on alternating-direction implicit method. *Microwave Theory and Techniques, IEEE Transactions on 47*, 1999, 2003–2007.

Peaceman D.W. & Rachford H.H.J. The numerical solution of parabolic and elliptic differential equations. *J Soc Ind Appl Math* 1955, **3**, 28–41.

Rogers B.D., Borthwick A.G.L. & Taylor P.H. Mathematical balancing of flux gradient and source terms prior to using Roe's approximate Riemann solver. *Journal of Computat Phys* 2003, **192**, 422–451.

Stelling G., Wiersma A. & Willemse J. Practical aspects of accurate tidal computations. *J Hydraulic Eng* 1986, **112**, 802–816.

Strang G. On the construction and comparison of difference schemes. *SIAMJ Numer Anal* 1968, **5**, 506–517.

Tayefi V., Lane S.N., Hardy R.J. & Yu D. A comparison of one- and two-dimensional approaches to modelling flood inundation over complex upland floodplains. *Hydrol Proc* 2007, **21**, 3190–3202.

Umgiesser G. & Zampato L. Hydrodynamic and salinity modeling of the Venice channel network with coupled 1-D–2-D mathematical models. *Ecol Modell* 2001, **138**, 75–85.

Vacondio R., Dal Palù A. & Mignosa P. GPU-enhanced Finite Volume Shallow Water solver for fast flood simulations. *Environ Model Softw* 2014, **57**, 60–75.

Villanueva I. & Wright N.G. Linking Riemann and storage cell models for flood prediction. *Proceedings of the ICE – Water Management*, 2006, pp. 27–33.

Werner M.G.F. Impact of grid size in GIS based flood extent mapping using a 1D flow model. *Physic Chem Earth, Part B: Hydrol, Oceans and Atmosphere* 2001, **26**, 517–522.

Wicks J., Syme B., Hassan M.A.A.M., Lin B. & Tarrant O. 2D modelling of floodplains – is it worth the effort? *Proceedings*

Journal of Flood Risk Management published by The Chartered Institution of Water and Environmental Management and John Wiley & Sons Ltd

of the River and Coastal Flooding Conference. Defra, UK, 2004, pp. 1–10.

Yu D. & Lane S.N. Urban fluvial flood modelling using a two-dimensional diffusion-wave treatment, part 1: mesh resolution effects. *Hydrol Proc* 2006a, **20**, 1541–1565.

Yu D. & Lane S.N. Urban fluvial flood modelling using a two-dimensional diffusion-wave treatment, part 2: development of a sub-grid-scale treatment. *Hydrol Proc* 2006b, **20**, 1567–1583.